BB

INS Report

INS-Rep.-1180
Dec. 1996

A step-like rise in the ^{4}He(γ,pn)^{2}H cross section near the pion-production threshold

K. Maruyama, K. Niki, Y. Sumi, T. Emura, I. Endo, S. Endo,
H. Itoh, S. Kato, M. Koike, K. Maeda, T. Maki, Y. Murata,
C. Rangacharyulu, A. Sasaki, T. Suda, Y. Wada, and K. Yoshida
(TAGX Collaboration)

CERN LIBRARIES, GENEVA
SCAN-9702018

SW9706

(To be published in Physics Letters B.)

Institute for Nuclear Study
University of Tokyo
Tanashi, Tokyo 188, Japan

A step-like rise in the $^4He(\gamma,pn)^2H$ cross section near the pion-production threshold

K. Maruyama, [1),a)] K. Niki, [2),1)], Y. Sumi,[2)] T. Emura,[3)] I. Endo,[2)] S. Endo,[2),b)]
H. Itoh,[4)] S. Kato, [1)] M. Koike, [1)] K. Maeda,[5)] T. Maki,[6)] Y. Murata, [1),c)]
C. Rangacharyulu,[7)] A. Sasaki,[8)] T. Suda,[5)] Y. Wada,[9)] and K. Yoshida[1),2)]

(TAGX Collaboration)

[1)] *Institute for Nuclear Study, University of Tokyo, Tanashi, Tokyo 188, Japan*

[2)] *Department of Physics, Hiroshima University, Hiroshima 730, Japan*

[3)] *Department of Applied Physics, Tokyo University of Agriculture and Technology, Koganei, Tokyo 184, Japan*

[4)] *Department of Physics, Saga University, Saga 840, Japan*

[5)] *Department of Physics, Tohoku University, Sendai 980-77, Japan*

[6)] *University of Occupational and Environmental Health, Kitakyushu 807, Japan*

[7)] *Department of Physics, University of Saskatchewan, Saskatoon S7N0W0, Canada*

[8)] *College of General Education, Akita University, Akita 010, Japan*

[9)] *Meiji College of Pharmacy, Setagaya, Tokyo 154, Japan*

(Received

[a] E-Mail address: maruyama@insuty.ins.u-tokyo.ac.jp; Fax number +81-424-62-0775.

[b] Present address: Research Institute for Radiation Biology and Medicine, Hiroshima University, Hiroshima 731-51, Japan.

[c] Present address: Musashino Women's College, Hoya, Tokyo 202, Japan.

Abstract

A kinematically complete $^4He(\gamma,pn)^2H$ measurement was carried out in the photon energy (E_γ) range 145 ~ 425 MeV. The total cross section (σ_α) forms a prominent structure whose peak lies at E_γ ~245 MeV (the *pnd* invariant mass of 3960 MeV/c^2). The ratio, σ_α/σ_d, where σ_d is the deuteron photodisintegration cross section, shows a step-like rise to a value of 6 at E_γ ~ 140 MeV.

PACS: 25.20.Lj; 25.10.+s; 25.20.Dc; 27.10.+h

Keywords: Step-like rise; Photodisintegration; Photon absorption; ^4He; Δ resonance; *pn* pair

As a result of extensive experimental and theoretical studies of deuteron photodisintegration [1], the photon-deuteron interaction is becoming understood in the photon energy (E_γ) range up to above the $\Delta_{33}(1232)$ resonance. The dominant theoretical ingredients in the non-relativistic formalism are the one-body nucleon current, meson-exchange currents, and the ΔN -transition current describing the photon-Δ excitation. Comparing with cross section data, one can select favorable NN potentials which determine the deuteron wave function. A TAGX experiment for three-body ^{3}He photodisintegration found that the photon-absorbing cross section by *pn* pairs in ^{3}He is 1.24±0.26 times larger than that for the deuteron [2]. Wilhelm et al. [3] successfully reproduce the data using a quasifree two-body model, in which the *pn* pair (0.5 pair in a nucleus) is three times more active in absorbing the photon due to its smaller size than the free deuteron.

We proposed to study photodisintegration of ^{4}He in order to determine the strength for photon absorption by the *pn* pairs in that nucleus. ^{4}He was selected because 1) it is one of the simplest nuclei whose ground-state wave functions can be reasonably well calculated, and 2) complete final-state identification is possible using TAGX. Inclusive (γ,*p*) and (γ,*pn*) measurements have been made [4,5], but they are not sufficient to specify the final state in the several-hundred-MeV E_γ region. Coincidence experiments of both (γ,*pn*) and (γ,*pp*) with the tagged photon are required to identify the *pnd* and *ppnn* final states.

The ^{4}He-photodisintegration processes, that are the dominant photon-absorbing mechanisms as well as that by GDRs below the pion-production-threshold energy, have sizable cross sections even in the Δ region as it was shown for the four-body breakup channel, *ppnn* [6]. Recently, Doran et al. [7] measured ^{4}He(γ, *pn*) ^{2}H, ^{4}He(γ, *pp*)*nn*, and ^{4}He(γ, *pn*)*pn* below the π threshold. The *pnd* data are accounted for by a mechanism of photon absorption on correlated *pn* pairs. That study motivated us to look at correlated *pn* pairs with the photodisintegration method at higher E_γ.

This experiment measured the three- and four-body ^{4}He breakup reactions in the E_γ range 145~425 MeV, which covers the entire Δ-resonance region. This letter presents the first total

cross section measurement for ^{4}He(γ,*pn*)^{2}H in the E_γ range and a prominent peak structure observed.

The present experiment was carried out using the TAGX spectrometer in the 20%-duty-cycle tagged-photon beam line at the 1.3-GeV Electron Synchrotron (ES) of INS, University of Tokyo. TAGX [8] is comprised of two parts: a π-sr solid-angle magnetic momentum analyzer for charged particles and a 0.85-sr solid-angle Time-Of-Flight (TOF, 300 ps time resolution) momentum analyzer for neutrons. The magnetic part consists of inner (IH) and outer (OH) plastic-scintillation counter hodoscopes used for both TOF measurement (350 ps resolution) and triggering, and two semi-cylindrical-shape eleven-layer drift chambers (CDC), which are sandwiched between the IH and OH and situated in a 5 kG vertical magnetic field. The TOF part consists of thick (10 and 30 cm) plastic scintillation counters with thin (1 cm) vetos in front. There were two kinds of triggering logic : 1) one charged particle in coincidence with a neutron (*pn*-mode) and 2) two charged particles (*pp*-mode). The triggering efficiency, which was a ratio of the number of successfully triggered events to that of detected ones, was computed by a Monte Carlo simulation to be 93% and 68% for *pn* and *pp*, respectively [9]. The larger inefficiency for *pp* came from the requirement of discarding those events in which both protons went into the same beam-left or -right hemispheres. Experimental details concerning the cryogenic ^{4}He target [10], trigger and data acquisition [9], and a general description of TAGX [8,11] have been fully described elsewhere.

The measurement was carried out as follows: a tagged photon beam (5-MeV rms energy resolution, 5 x 10^5 γ/s) hit the liquid ^{4}He target contained in a vertically installed cylindrical Mylar (125 μm thick) cell 5 cm in diameter. Charged particle momenta were measured in the angular range 15 ° ~165 ° by the curvatures of the reconstructed trajectory with resolution expressed by $\Delta p/p = 9\times10^{-5}\,p + 0.01$ (p in MeV/c). The momentum was calibrated to the momentum analyzed (0.3% resolution) electron beams from the ES. Protons, whose momentum were required to be greater than 300 MeV/c, were selected from the positively-

charged track sample by using TOF and the reconstructed momentum with a purity of better than 97%.

Neutron momenta and emission angles were measured in the range of 100 ~ 800 MeV/c with 2 ~ 10% resolution and 18 ° ~162 ° with 2.0° resolution, respectively. Charged particle hits on the counter were removed by the use of both the vetos and/or charged-particle-track extrapolation from the CDC. The 5-MeV (electron equivalent) threshold energy for the neutron was calibrated with radioactive sources during the run. Photon hits were rejected by cuts in the TOF spectrum.

Overall performance of the tagged-photon beam and TAGX system in kinematical event reconstruction was examined by measuring the H(γ,π^+n) reaction. The photon energy, the π^+ momentum vector, and the neutron momentum vector were proved to be consistently reconstructed within resolution limits. The differential cross section data for H(γ,π^+n), which are consistent with existing data, confirmed our capability in obtaining absolute cross sections.

Both of the *pn*- and *pp*-mode events were analyzed on an event-by-event basis. Non-target background was rejected by applying cuts to the reaction vertex point which was reconstructed in two ways: for the *pp*-mode event, it was defined as the closest approach between two proton trajectories, and for the *pn*-mode event, the distance between the proton trajectory and the target center was used. The ratio of the empty-target yield to full-target yield was measured to be (18.2±0.5)% for the *pn*-mode and (20.0±1.4)% for the *pp*-mode, and the empty yields were subtracted from the full yields. The numbers of events remaining after the subtraction were 14400 of *pn*-mode for 2.05 x 10^{11} photons and 3700 of *pp*-mode for 1.01x10^{11} photons.

The missing masses of pnX and ppX, where X represents a system of unobserved particles, were computed by using E_γ and the reconstructed momenta. Since pnX comes from both *pnd* and *ppnn*, and ppX comes from *ppnn* only, the yield difference between pnX and ppX, after being corrected for the detector acceptance, is the contribution from *pnd*. While the missing mass spectrum for ppX shows a smooth background behavior over the kinematically

allowed region, the spectrum for pnX shows a peak at the deuteron mass in addition to the background behavior.

The *pnd* yield was determined in such a way which follows. The missing mass spectrum for ppX was subtracted from that for pnX. Normalization of ppX was determined by taking into account the differences for *pp*(*nn*) and *pn*(*pn*) in detector acceptances, which were computed using a three-body photon-absorption model that describes the four-body breakup channel [12]. Here, we assume that the four-body breakup spectra for the *pn*-mode and the *pp*-mode are the same, what is justified in an example shown in Fig. 1. The subtracted spectrum below 2000 MeV/c^2 shown in Fig. 1 is reproduced by a gaussian curve whose peak lies at 1876±3 MeV/c^2 with a mass width Δm = 45±3 MeV/c^2, which are consistent with the deuteron mass and the E_γ-dependent detector resolution, respectively. To exclude single-pion production contribution, we did not deal with those events whose missing masses were greater than $2m_N + m_\pi - \Delta m$, where m_N is the nucleon mass and m_π the pion mass.

A simulation code (TAGX-FMC) was used in order to reproduce experimentally obtained momentum spectra for each of the ^{4}He(γ, *pn*) ^{2}H, ^{4}He(γ,*pp*)*nn*, and ^{4}He(γ, *pn*)*pn* reactions as a function of E_γ. The code consists of an event-generator part and a detector-simulator part. Particles, whose momentum vectors are given by a model generator, are produced in the target by the photon, and are tracked into the detector. Each of the produced particles in the detector gives a trajectory obtained by taking into account the energy-momentum of the particle, the non-uniform magnetic field distribution, the effects of Coulomb multiple scattering, ionization energy losses and nuclear interactions. The trajectory gives a set of simulated signals for all detector components by taking into account of their geometry, resolution and efficiency. Track reconstruction and kinematical event reconstruction are performed for the simulated events in the same way as for the real events.

The *pnd* events were accumulated in bins of the five-dimensional space defined by the proton and neutron momenta (25 MeV/c in width), the proton and neutron polar angles (20 ° in width), and the relative azimuthal angle between the proton and the neutron (20° in width).

The number of all bins is 2×10^5. The *pnd* yield in a bin j is denoted by Y_j. The formula used for the total cross section (σ) determination is:

$$\sigma = \frac{1}{N_\gamma \cdot N_T \cdot \alpha} \sum_j \frac{Y_j}{\varepsilon_j}, \qquad (1)$$

where N_γ is the number of incident photons, N_T the number of target nuclei, and Σ_j denotes the sum over all the bins. The correction factors α and ε represent the overall unobserved-yield correction and the detection-efficiency correction in each bin, respectively. The factor α depends on the reaction model used, while ε does not.

The magnitude of ε in each bin was determined using the code TAGX-FMC. Events with two particles (*pp* or *pn*), which were generated in random directions with random magnitudes of momentum assigned to the appropriate bin, and those which were detected were counted. The ratio of the detected to generated events in a bin j is defined as ε_j. The geometrical solid angle and the detection efficiency of the detector for the bin are therefore included in this factor. Any bins of vanishingly small ε (proton momentum less than 300 MeV/c, for example) are not included in the summation to avoid overly large efficiency corrections.

The factor α corrects for the contribution from such avoided (unobserved) kinematical regions. To investigate the dependency of α on the reaction model, we considered several photon absorption models. It was found that the factor is not sensitive to the absorption model used as far as the model reproduces the momentum and angular distributions of the observed proton and neutron. A two-body absorption model was used. The value of α is 0.7 at 150 MeV, 0.85 at 200 MeV, and it becomes close to unity at higher E_γ. This is reasonable because TAGX is more efficient at detecting protons of higher energy.

The systematic uncertainties in the yield determination by the event reconstruction, in the detection efficiency computations and in various corrections applied to obtain the total cross section have been estimated. The uncertainty in the incident photon flux is 6%, that of the target

thickness is 3%, yield determination for *pnd* of 7% and for *ppnn* of 6%, dead time correction of 1%, and detection efficiency for *pnd* of 5~10% and *ppnn* of 30~50%. The quadratic sum of systematic uncertainties are 11% for *pnd* and 32~51% for *ppnn*.

The total cross section for ^{4}He(γ,*pn*)^{2}H obtained as a function of E_γ is shown in Fig. 2. The E_γ dependence forms a broad peak centered at 245 MeV, and it drops steeply down to 10% of the peak cross section at 415 MeV. The dependence is similar to that of deuteron photodisintegration in shape, but the cross section is 6 times larger in magnitude. For the deuteron photodisintegration, there are several theoretical calculations. Arenhövel et al. [1] include the $M1$ transition due to the Δ in addition to $E1$, while the higher multipoles contribute much less than 10%. If one assumes the same dominant electromagnetic currents in ^{4}He as those in the deuteron, it can be concluded that both strengths of $M1$ and $E1$ transitions are 6 times larger in ^{4}He than in the deuteron. When one takes into account of the effective number of the *pn* pairs in ^{4}He, which is given to be ~2.4 by Schiavilla et al. [13], an additional factor of 2.5 enhancement in the photon-absorbing strength is required to match the data, presumably due to the difference of the wave functions.

Photodisintegration of the quasifree *pn* system in nuclei was observed by Homma et al. in the proton inclusive measurement on ^{9}Be [14], and on ^{4}He [4]. Their differential cross sections for ^{4}He(γ,*p*) (a sum of *pnd* and *ppnn*) give a ^{4}He to ^{2}H ratio of 4.5, which is lower than the present experiment but still marginally consistent. A theoretical calculation by Tezuka [15], who assumes the photodisintegration mechanism of the strongly correlated *pn* pairs in the nucleus, describes well the data by Homma et al. [4], and it reproduces the present data qualitatively as shown in Fig. 2.

The peak position corresponds to the c.m. energy (the *pnd* invariant mass M) of 3960 MeV/c^2, which is 86 MeV/c^2 lower than the sum of the masses of three nucleons and one Δ (m_Δ); $M = 3m_N + m_\Delta - 86$ (MeV/c^2). The relation can be rewritten in another way; $M = m_\alpha + (m_\Delta - m_N) - 61$ (MeV/c^2), where m_α is the mass of ^{4}He. If one can assume that the peak structure is

due to Δ excitation of one nucleon in ^{4}He, the relation allows a speculation that a $NNN\Delta$ state is formed as a whole, with the separation energy of the Δ being 61 MeV/c^2.

Four experiments of three-body breakup have been carried out at Lebedev [16], Ukraine [17], Torino [18], and Mainz [7], whose data are also shown in Fig. 2. The former three measured ^{4}He(γ,*pd*)*n* with mutually similar experimental methods: a bremsstrahlung γ beam hit a compressed-gas ^{4}He target to break the nucleus into *pnd*, and both of *p* and *d* were measured with a cloud chamber which was placed in a magnetic field. The three sets of data, although they have large statistical errors, share a common E_γ dependence: they rise steeply from the reaction threshold to a peak of 200 μb at around 40 MeV, then they decrease slowly down to 40 μb at 140 MeV. The measurement at Mainz by Doran et al. [7] with tagged photons of energies 80~131 MeV detected *pn*, and determined the *pnd* final state by the missing energy method. This is the same as the present experiment in method. Their total cross section data presented are not inconsistent with the earlier data in magnitude, but the increasing E_γ dependence observed is different from decreasing tendency of the others. A theoretical calculation by Noguchi and Prats [19], which is based on the quasi-deuteron model, reproduces the gross features made of the four data sets.

A direct comparison between these data at lower energies and the present data can be made only in the overlapping region at around 140 MeV. The present data at 155±10 MeV is ten times larger than the data at 100~170 MeV by Gorbunov et al. [16]. Figure 3 shows a plot of the total cross section (σ_α) divided by the total cross section for deuteron photodisintegration (σ_d) [20]. It shows a constant behavior with the values of 0.5~1.5 at energies below 140 MeV, and also a constant behavior at higher energies above 140 MeV with the value of 6.0±0.3. This indicates that the effective number of the photon-absorbing *pn* pairs in ^{4}He changes very steeply at ~140 MeV. This step-like rise occurs at an energy very close to the π-production threshold on one of the nucleons. It may suggest an opening of a reaction mechanism which is not yet established. We could find no experimental cause to induce such a normalization error much greater than the estimated systematic errors. We have published the results of the total

cross section of four-body-breakup channel ^{4}He (γ,*ppn*)*n* [6] obtained in a kinematically complete way at energies of 145~425 MeV [12]. The cross section ratio of the four-body-breakup to the three-body-breakup increases linearly as a function of E_γ, and it takes the maximum of 25% at 400 MeV. Therefore, systematic errors of 32~51% for the four-body-breakup do not explain the rise.

π^+ absorption experiments in ^{4}He have been used to determine the number of isoscalar *pn* pairs in the nucleus. The result is 2.9 ± 0.5 in the pion kinetic energy range 100 ~ 500 MeV [21,22,23,24]. This is consistent with the present result of 6 at higher E_γ, if one relies on the Δ-hole calculation which estimates the reduction in the number due to the initial state interaction to be ~50% [25]. At 65 MeV, a significantly smaller number of 1.74 ± 0.42 was reported [22]. It is worth noting that this change seems to be consistent with the present step-like rise.

In conclusion: A new kinematically complete measurement of ^{4}He (γ,*pn*) ^{2}H at E_γ =145 ~ 425 MeV identifies the photon-absorbing *pn* pairs in ^{4}He. The total cross section, σ_α, which determines the absorbing strength, shows a broad prominent peak structure at the *pnd* invariant mass of 3960 MeV/c^2. The ratio, σ_α / σ_d, exhibits a constant behavior with the value of 1.0±0.5 below 140 MeV, but with the value of 6.0±0.3 in the range above 140 MeV. A constant behavior, which comes from the similarity in the photon-absorbing mechanisms (*E*1 and *M*1 transitions) by the bound *pn* system and the free deuteron, is plausible. On the contrary, the step-like change, which is much more significant than the systematic errors, in the total cross section at the π−production threshold is explained by no known mechanism. A similar, although not well established, change in the ratio of π^+ absorption in ^{4}He to that in the deuteron might also be a clue to understand this. If there were unbound *pn* systems of which invariant masses are close to the deuteron mass, they might be included in the *pnd* yield and cause the rise. A better-resolution measurement in future is desirable to confirm the present rise.

We would like to express our sincere thanks to Prof. S. Yamada and Prof. H. Okuno for their encouragement of this work. We appreciate Dr. G. Garino for his critical comments to the manuscript. Thanks are due to the ES crew for their support in carrying out the experiment. Part of this work is financially supported by the Grant-in-Aid for Special Project Research on Meson Science of the Ministry of Education, Science, Sports and Culture of Japan.

References

[1] H. Arenhövel and M Sanzone, Few-Body Systems **Suppl. 3**(1991)1.

[2] T. Emura et al. (TAGX Collab.), Phys. Rev. **C49**(1994)R597.

[3] P. Wilhelm, J.A. Niskanen and H. Arenhövel, Phys. Lett. **B335**(1994)109.

[4] S. Homma et al., Phys. Rev. **C36**(1987)1623.

[5] M.Q. Barton and J.H. Smith, Phys. Rev. **110**(1958)1143.

[6] T. Emura et al. (TAGX Collab.), Phys. Lett. **B286**(1992)229.

[7] S.M. Doran et al., Nucl. Phys. **A559**(1993)347.

[8] K. Maruyama et al. (TAGX Collab.), Nucl. Instrum. Methods **A376**(1996)335.

[9] K. Niki et al., Nucl. Instrum. Methods **A294**(1990)534.

[10] S. Kato et al., Nucl. Instrum. Methods **A290**(1990)315.

[11] K. Niki, J. Sci. Hiroshima Univ., **55A**(1991)53.

[12] T. Emura et al. (TAGX Collab.), Phys. Lett. **B267**(1991)460.

[13] R. Schiavilla, V.R. Pandharipande and R.B. Wiringa, Nucl. Phys. **A449**(1986)219.

[14] S. Homma et al., Phys. Rev. Lett. **45**(1980)706.

[15] H. Tezuka, J. Phys. Soc. Japan **57**(1988)3766.

[16] A.N. Gorbunov and V.M. Spridinov, Sov. Phys. JETP **34**(1958)600; A.N. Gorbunov, Sov. J. Nucl. Phys. **10**(1969)268; Proc. P.N. Lebedev Phys. Inst. **71**(1974)1.

[17] Yu. A. Arkatov et al., JETP Lett. **9**(1969)278; Sov. J. Nucl. Phys. **10**(1970)639.

[18] F. Balestra et al., Nuovo. Cim. **49A**(1979)575; F. Balestra et al., Nuovo. Cim. **38A**(1977)145.

[19] C.T. Noguchi and F. Prats, Phys. Rev. **C14**(1976)1133.

[20] P. Rossi et al., Phys. Rev. **C40**(1989)2412.

[21] R.D. McKeown et al., Phys. Rev. **C24**(1981)211.

[22] M. Steinacher et al., Nucl. Phys. **A517**(1990)413.

[23] F. Adimi et al., Phys. Rev. **C45**(1992)2589.

[24] L.C. Smith et al., Phys. Rev. **C48**(1993)R485.

[25] K. Ohta, M. Thies and T.-S. Lee, Ann. Phys. **163**(1985)420.

Figure captions

Fig. 1 The missing mass spectrum for *pnX* (solid circles) in the E_γ range 285~325 MeV is reproduced by a sum of *pnd* and *pnpn* (solid curve). The detector-acceptance corrected *ppX* spectrum (open circles) and the calculated *pnpn* curve (dot-dashed curve) show a good agreement. The difference between *pnX* and the *ppX* is represented by a gaussian whose peak lies at the deuteron mass. This confirms that the main contributor to the *pnX* yield is three-body breakup, *pnd*. Events above 2011 MeV/c^2 include pion production.

Fig. 2 The total cross sections for $\gamma\ ^4\mathrm{He} \rightarrow pnd$. Solid circles are the present result. The dashed curve is a fit to $\sigma(^2\mathrm{H}(\gamma,pn))$ [20], and the dotted curve is a theoretical calculation by Tezuka [15]. Data at lower energies are from Gorbunov et al. [16], Arkatov et al. [17], Balestra et al. [18], and Doran et al. [7].

Fig. 3 The ratio of $\sigma(^4\mathrm{He}(\gamma,pnd)) / \sigma(^2\mathrm{H}(\gamma,pn))$ as a function of E_γ. Solid circles are the present data. The data at lower energies are from Gorbunov et al. [16], Arkatov et al. [17], and Doran et al. [7]; ref. 18 is not used to avoid confusion in the plot, but is not significantly different. The reaction threshold and π-production threshold are indicated by arrows.

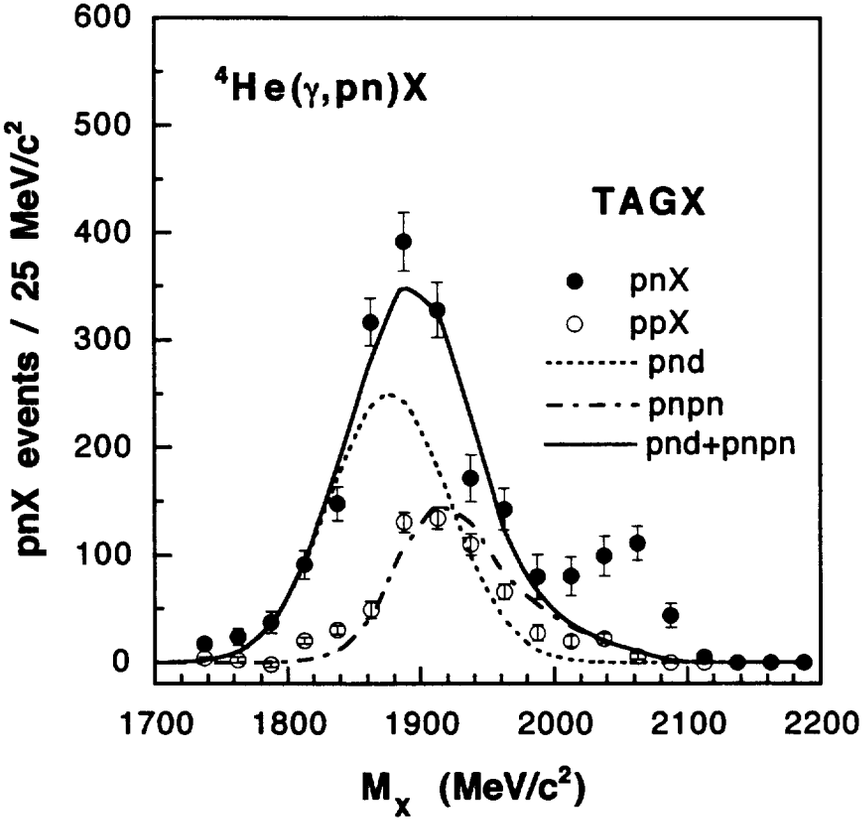

Fig. 1

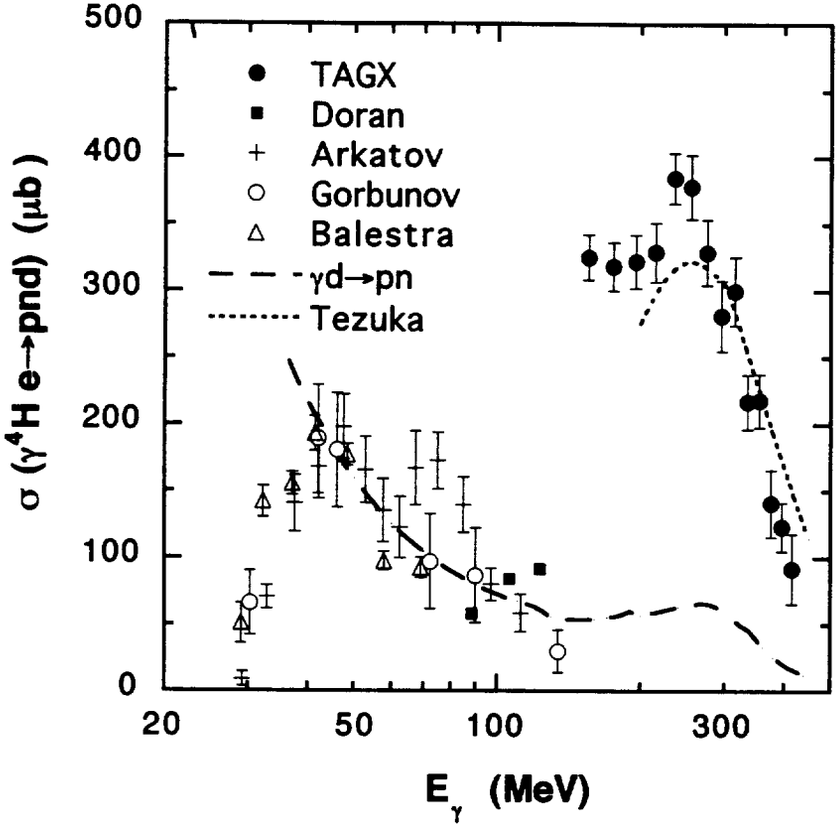
TAGX
Doran
Arkatov
Gorbunov
Balestra
γd→pn
Tezuka
σ (γ⁴H e→pnd) (μb)
E_γ (MeV)

Fig. 2

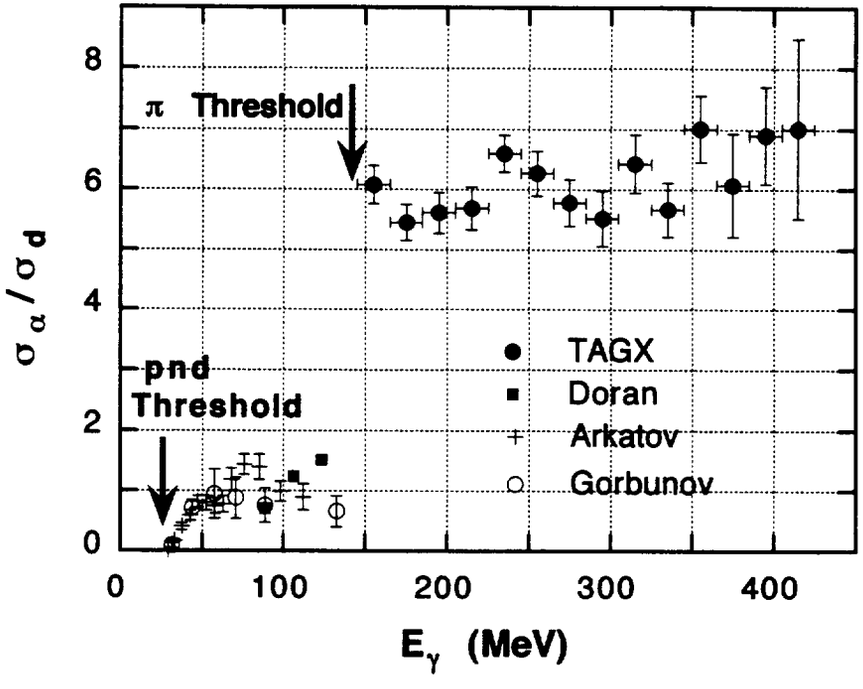
π Threshold
pnd Threshold
TAGX
Doran
Arkatov
Gorbunov
σ_α / σ_d
E_γ (MeV)

Fig. 3